Distance Dependence of the Low-Temperature Electron Transfer Kinetics of (Ferrocenylcarboxy)-Terminated Alkanethiol Monolayers

Michael T. Carter, Gary K. Rowe, John N. Richardson,† Leonard M. Tender,‡ Roger H. Terrill, and Royce W. Murray*

Contribution from the Kenan Laboratories of Chemistry, University of North Carolina, Chapel Hill, North Carolina 27599-3290

Received September 26, 1994®

Abstract: Results are presented for rate constants ($k°$) and reorganizational energy barriers (λ) for interfacial electron transfer at ultralow-temperatures (120−150 K) across mixed $CpFeCpCO_2(CH_2)_nSH/CH_3(CH_2)_{n-1}SH$ monolayers (n = 8, 12, 16). The monolayers are kinetically disperse, i.e., the ferrocene sites exhibit a range of rate constants. Average values of $k°$ were measured by cyclic voltammetry with application of Marcus theory corrected for the density of electronic states in the gold electrode. The $k°$ and pre-exponential (μQ) values exhibit exponential dependencies on alkane chain length characterized by exponential coefficients of 1.06 and 1.44/CH_2, respectively. The former value agrees with aqueous phase results by others for analogous but more highly ordered monolayers near ambient temperatures; the latter result corresponds to an electronic coupling coefficient of β_{EL} of 1.1 $Å^{-1}$. The activation analysis-derived reorganizational barrier energies decrease somewhat with increasing chain length, contrary to theoretical expectations.

Introduction

We describe here the temperature and distance dependence of low-temperature (120−150 K) electron transfer rate constants ($k°$) in a cryoelectrochemical solvent mixture[1] (EtCl/PrCN) for self-assembled mixed monolayers (SAM's) of the ferrocene alkanethiol $CpFeCpCO_2(CH_2)_nSH$ (Cp = cyclopentadienyl) and n-alkanethiol $CH_3(CH_2)_nSH$ cochemisorbed[2] on etched Au electrodes. Elucidating distance-dependent electronic coupling between electrode and redox sites is of interest both for mechanistic reasons and for learning how to predictably tune interfacial electron transfer rates. The structural order of alkanethiol monolayers makes them attractive for this purpose. There are few existing examples[3-5] of distance-dependent studies using self-assembled redox active monolayers, and most have been done in aqueous electrolytes. There have been numerous studies of structure- and distance-dependent electron transfer in solutions, using donors and acceptors separated by rigid structures,[6,7] that have led to important insights and theory for through-bond coupling of the electron transfer event.

Our low-temperature investigations[8] of ferrocene alkanethiol monolayers in the EtCl/PrCN solvent[1] have revealed that $k°$ varies among the SAM ferrocene site populations; i.e., $k°$ exhibits a kinetic dispersion. Such kinetic dispersion, absent in the initial report by Chidsey,[9] has been seen by others[4,10] in redox active alkanethiol monolayers. For a given monolayer, the dispersion appears to be less in aqueous vs nonaqueous solvents, and in the PrCN/EtCl solvent the dispersion increases at lowered temperatures.[8b,e] Kinetic heterogeneity is in fact common for electron transfers in media that are effectively rigid on the electron transfer timescale;[11] for example it has been discussed by Gudowska-Nowak[12] to explain experimentally observed inhomogeneous line broadening and nonexponential fluorescence decay in donor−acceptor molecules undergoing photochemically-induced electron transfers. Kinetic dispersion complicates measurements of $k°$ by potential step methods,[8c,d]

† Present address: Department of Chemistry, Shippensburg University, Shippensburg, PA 17257.

‡ Present address: Department of Chemistry, Stanford University, Stanford, CA 94305.

® Abstract published in *Advance ACS Abstracts*, February 15, 1995.

(1) Ching, S.; McDevitt, J. T.; Peck, S. R.; Murray, R. W. *J. Electrochem. Soc.* **1991**, *138*, 2308.

(2) Chidsey, C. E. D.; Bertozzi, C. R.; Putvinski, T. M.; Mujsce, A. M. *J. Am. Chem. Soc.* **1990**, *112*, 4301.

(3) (a) Dubois, L. H.; Nuzzo, R. G. *Annu. Rev. Phys. Chem.* **1992**, *43*, 437; β = 1.07/CH_2. (b) Chidsey, C. E. D. Presented at the C. N. Reilley Symposium. Pittcon94, Chicago, IL, March 1994; β = 1.11/CH_2. (c) Feldberg, S. W. Seminar. University of NC, February, 1994; β = 1.21/CH_2.

(4) Finklea, H. O.; Hanshew, D. D. *J. Am. Chem. Soc.* **1992**, 114, 3173.

(5) (a) Becka, A. M.; Miller, C. *J. Phys. Chem.* **1992**, *96*, 2657. (b) Li, T. T.-T.; Weaver, M. J. *J. Am. Chem. Soc.* **1984**, *106*, 6107. (c) Forster, R. J.; Faulkner, L. R. *J. Am. Chem. Soc.*, **1994**, *116*, 5444; 5453.

(6) (a) Newton, M. D. *Chem. Rev.* **1991**, *91*, 767. (b) Beratan, D. N.; Hopfield, J. J. *J. Am. Chem. Soc.* **1984**, *106*, 1584. (c) Closs, G. L.; Calcaterra, L. T.; Green, N. J.; Penfield, K. W.; Miller, J. R. *J. Phys. Chem.* **1986**, *90*, 3673. (d) Jordan, K. D.; Paddon-Row, M. N. *Chem. Rev.* **1992**, *92*, 395. (e) Ratner, M. A. *J. Phys. Chem.* **1990**, *94*, 4877. (f) Koga, N.; Sameshima, K.; Morokuma, K. *J. Phys. Chem.* **1993**, *97*, 13117. (g) Haran, A.; Waldeck, D. H.; Naaman, R.; Moons, E.; Cahen, D. *Science* **1994**, *263*, 948. (h) Broo, A.; Laisson, S. *Chem. Phys.* **1990**, *148*, 103.

(7) (a) Casimiro, D. R.; Richards, J. H.; Winkler, J. R.; Gray, H. B. *J. Phys. Chem.* **1993**, *97*, 13073. (b) Casimiro, D. R.; Wong, L. L.; Colon, J. L.; Zewert, T. E.; Richards, J. H.; Chang, I. J.; Winkler, J. R.; Gray, H. B. *J. Am. Chem. Soc.* **1993**, *115*, 1485. (c) Isied, S. S.; Ogawa, M. Y.; Wishart, J. F. *Chem. Rev.* **1992**, *92*, 381. (d) McLendon, G.; Hake, R. *Ibid.* **1992**, *92*, 481. (e) Wuttke, D. S.; Bjerrum, M. J.; Winkler, J. R.; Gray, H. B. *Science* **1992**, *256*, 1007.

(8) (a) Curtin, L. S.; Peck, S. R.; Tender, L. M.; Murray, R. W.; Rowe, G. K.; Creager, S. E. *Anal. Chem.* **1993**, *65*, 386. (b) Tender, L. M.; Carter, M. T.; Murray, R. W. *Anal. Chem.* **1994**, 66, 3173. (c) Richardson, J. N.; Peck, S. R.; Curtin, L. S.; Tender, L. M.; Terrill, R. H.; Carter, M. T.; Murray, R. W.; Rowe, G. K.; Creager, S. E. *J. Phys. Chem.*, in press. (d) Richardson, J. N.; Rowe, G. K.; Carter, M. T.; Tender, L. M.; Curtin, L. S.; Peck, S. R.; Murray, R. W. *Electrochim. Acta*, in press. (e) Rowe, G. K.; Carter, M. T.; Richardson, J. N.; Murray, R. W. *Langmuir*, submitted.

(9) Chidsey, C. E. D. *Science* **1991**, *251*, 919.

(10) Ravenscroft, M. S.; Finklea, H. O. *J. Phys. Chem.* **1994**, *98*, 3843.

(11) (a) Kinetic dispersity in amorphous polymeric films that are electron-conductive by a hopping mechanism is well-known.[11b-d] (b) Scher, N.; Montroll, E. W. *Phys. Rev. B* **1975**, *12*, 2455. (c) Pfister, G. *Phys. Rev. B* **1977**, *16*, 3676. (d) Sullivan, M. G.; Murray, R. W. *J. Phys. Chem.* **1994**, *98*, 4343.

(12) Gudowska-Nowak, E. *J. Phys. Chem.* **1994**, 98, 5257.

0002-7863/95/1517-2896$09.00/0

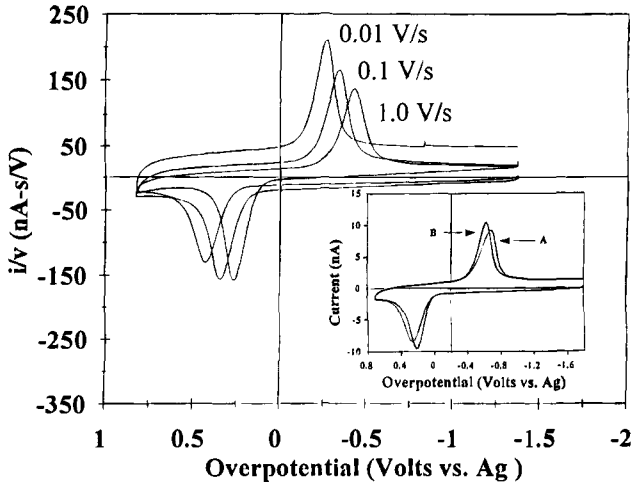

Figure 1. Sweep rate dependence of cyclic voltammetry for a $CpFeCpCO_2(CH_2)_{16}SH/CH_3(CH_2)_{15}SH$ monolayer on a gold disk electrode at 140 K. For the sweep rates indicated, the values of ΔE_{PEAK} are 527, 679, and 857 mV. Inset: comparison of (A) uncorrected and (B) instrumentally iR_{UNC}-corrected cyclic voltammograms (100 mV/s; 120 K, $\Gamma = 1.15 \times 10^{-10}$ mol/cm^2).

but we have found that cyclic voltammetric measurements[8b-d,13] give average $k°$ values for electroactive SAM's with minimal sensitivity[8e] to kinetic dispersion. This report presents results for $n = 8$, 12, and 16 SAM's that show the low-temperature $k°$ values to vary exponentially with alkane chain length even though the monolayers are kinetically polydisperse.

Experimental Section

Chemicals. $CpFeCpCO_2(CH_2)_nSH$ (Cp = cyclopentadienyl; n = 8, 12, 16) were available from previous studies.[8] Octanethiol, dodecanethiol, hexadecanethiol (Aldrich), HCl (Mallinckrodt), HNO_3 (EM Science), butyronitrile (PrCN, Aldrich, 99+ %), absolute ethanol (AAPER Alcohol and Chemical Co.), and tetra-*n*-butylammonium hexafluorophosphate (n-Bu_4NPF_6, Fluka, Puriss grade) were used as received. Ethyl chloride (EtCl, Linde) was condensed into a Schlenk tube and stored at room temperature. Water was purified with a Barnstead NANOpure system. Electrode fabrication, monolayer preparation, and electrochemical cell design are as described previously.[8]

Electrochemical Measurements. Cyclic voltammetry was carried out with a potentiostat of local construction and a microcomputer (Micro Systems Engineering 486) with a homemade program for potential control and data acquisition. A home built filter was employed to improve signal-to-noise (S/N), and a positive feedback control circuit effected instrumental positive feedback for uncompensated resistance correction. The uncompensated resistance correction allowable without circuit instability, estimable from the setting on the feedback compensation module, is generally near actual uncompensated resistance values measured by ac impedance in each experiment at the temperature of interest with a Schlumberger-Solartron Instruments Model 1255 frequency analyzer and Model 1286 potentiostat. The agreement of the two R_{UNC} values indicates a nearly full resistance compensation.

The potential scan rate dependency of the voltammetry of a mixed monolayer of $CpFeCpCO_2(CH_2)_{16}SH/CH_3(CH_2)_{15}SH$ on a gold disk electrode at 140 K is shown in Figure 1. The ΔE_{PEAK} separation between oxidation and reduction peak potentials increases with increasing potential scan rate, consistent with electron transfer rate control. Table 1 displays ΔE_{PEAK} results for $n = 16$ monolayers (Figure 1) as a function of temperature and scan rate, with $k°$ rate constants calculated (*vide infra*) from them. The $k°$ results are, within experimental error, independent of potential scan rate, which is a criterion for the absence of any substantial contribution of iR_{UNC} effects to the experimental ΔE_{PEAK} values.

(13) (a) Creager, S. E.; Weber, K. *Anal. Chem.* **1994**, 66, 3164. (b) Nahir, T. M.; Clark, R. A.; Bowden, E. F. *Anal. Chem.* **1994**, *66*, 2598.

Table 1. Cyclic Voltammetry Peak Potential Separations (ΔE_{PEAK}) and Marcus–DOS Derived Rate Constants for a $CpFeCpCO_2(CH_2)_{16}SH/CH_3(CH_2)_{15}SH$ SAM in Contact with 2:1 (v/v) Chloroethane:Butyronitrile/0.075 M Bu_4NPF_6

T/K[a]	v (V/s)	ΔE_{PEAK} (mV)	$k°$ (s^{-1})
120	0.01	647	2.0×10^{-6}
$\Gamma = 1.15 \times 10^{-10}$ mol/cm^2	0.1	810	2.5×10^{-6}
	1.0	1045	2.0×10^{-6}
130	0.01	586	1.1×10^{-5}
$\Gamma = 1.22 \times 10^{-10}$ mol/cm^2	0.1	742	1.3×10^{-5}
	1.0	950	1.4×10^{-5}
140	0.01	527	3.5×10^{-5}
$\Gamma = 1.44 \times 10^{-10}$ mol/cm^2	0.1	679	3.7×10^{-5}
	1.0	857	4.0×10^{-5}
150	0.01	476	1.1×10^{-4}
$\Gamma = 1.50 \times 10^{-10}$ mol/cm^2	0.1	630	1.4×10^{-4}
	1.0	805	1.5×10^{-4}

[a] The bulk gold disk area was 0.002 cm^2. Electroactive ferrocene surface coverages (Γ) were determined by integration of the cathodic branch of a 5 mV/s voltammogram at each temperature. The drift in the coverage values is an artifact due to problems of measuring the charge under the edges of the peak;[8a] the original coverage is recovered upon change in temperature.

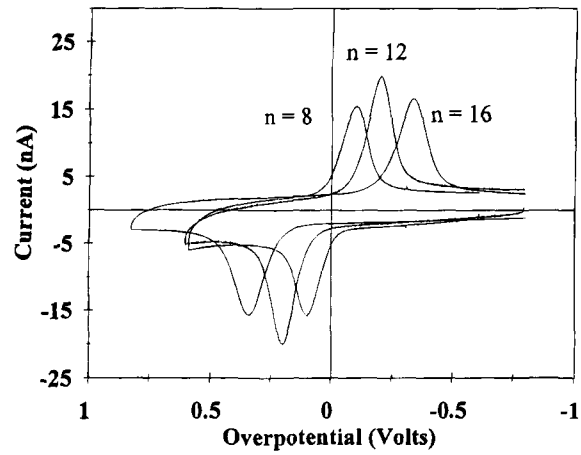

Figure 2. Cyclic voltammograms (v = 100 mV/s) of $CpFeCpCO_2(CH_2)_n$-$SH/CH_3(CH_2)_{n-1}SH$ monolayers on 0.002 cm^2 Au electrodes at 140 K in 2:1 EtCl:PrCN/0.075 M Bu_4NPF_6. Values of ΔE_{PEAK} are 96, 405, and 679 mV and ferrocene surface coverages are 1.3×10^{-10}, 1.6×10^{-10}, and 1.4×10^{-10} mol/cm^2 for n = 8, 12, and 16, respectively.

The inset in Figure 1 gives a further analysis of possible interference from iR_{UNC} at 120 K, which is the worst case situation in terms of solution ionic resistance. R_{UNC} is 1.6 MΩ by ac impedance spectroscopy at this temperature, which is a large value, but on the other hand, the currents are small (i_{PEAK} = 10 nA in the Figure 1 inset). The inset shows 100 mV/s (n = 16) ferrocene alkanethiol monolayer voltammograms evaluated with and without the application of instrumental positive feedback; these exhibit ΔE_{PEAK} = 810 and 949 mV, respectively. Use of the latter ΔE_{PEAK} value, containing a full iR_{UNC} effect, would depress the measured apparent $k°$ by about 5-fold. This is then roughly the size of the maximum possible error in $k°$ for the n = 16 monolayer under conditions of largest R_{UNC} (lowest temperature employed). With positive feedback we believe any actual error is much smaller and, given that $k°$ is invariant with scan rate, undetectable in the Table 1 data.

Results and Discussion

Cyclic voltammograms at 140 K for n = 8, 12, and 16 ferrocene SAM's (Figure 2) exhibit oxidation–reduction peak potential separations (ΔE_{PEAK}) that increase systematically (i.e., smaller $k°$) with increasing alkane chain length. Rate constants $k°$ were obtained from ΔE_{PEAK} values such as in Figures 1 and 2 and Table 1, taken as a function of potential sweep rate (v), using a Marcus theory formulation.[8b,13-15] The analysis involves

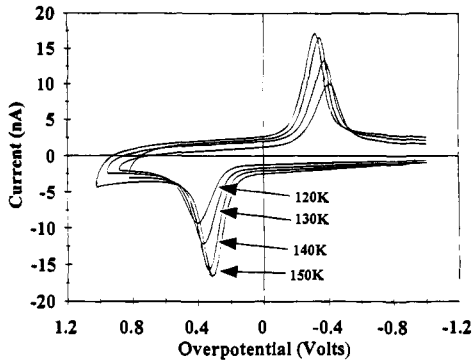

Figure 3. Temperature-dependent cyclic voltammetry (100 mV/s) of a mixed monolayer of $CpFeCpCO_2(CH_2)_{16}SH/CH_3(CH_2)_{15}SH$/bulk. The conditions are as in Table 1.

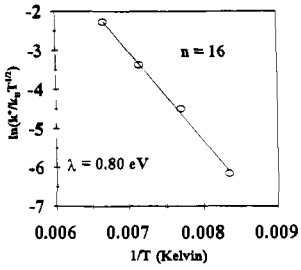

Figure 4. Activation plot for the temperature dependence of $k°$ for a monolayer of $CpFeCpCO_2(CH_2)_{16}SH/CH_3(CH_2)_{15}SH$. Reference 8c,d give analogous plots for $n = 8$ and 12.

digitally simulating voltammograms with Marcus-density of states theory[14] to generate working curves of ΔE_{PEAK} vs $\log(\nu/k°)$. These working curves and accordingly thus derived $k°$ values are not strongly sensitive[8b] to the value of electron transfer barrier reorganizational energy (λ) assumed in the working curve.

The temperature dependence[16] of cyclic voltammetrically-determined $k°$ values is used to measure λ. Figure 3 shows that the separation ΔE_{PEAK} between oxidation and reduction peak potentials in $CpFeCpCO_2(CH_2)_{16}SH/CH_3(CH_2)_{15}SH$ mixed monolayer voltammetry increases as the electron transfer rate is thermally quenched by lowered temperatures. Figure 4 shows an activation plot for the n = 16 ferrocene SAM. Values of λ and of the pre-exponential term[14] $\mu\varrho$ taken from this plot and from analogous plots for n = 8 and 12 described elsewhere[8c,d] are presented in Table 2. Also in Table 2 are theoretical predictions from the classical dielectric continuum theory[15,17] (λ_{CLASS}) and from a more recent two-dielectric-layer (λ_{2LAYER}) calculation[17c] made for ferrocene SAM's but in aqueous medium. (Since $\epsilon_{OP}(aq) = 1.8$ vs $\epsilon_{OP}(EtCl/PrCN, T = 125\ K) = 2.1$, the λ_{2LAYER} values given have been reduced by 10%.) From a comparison of experiment and theory in Table 2, there is good agreement with both theoretical values for $n = 16$, but for the shorter chains the experimental λ increases whereas theory predicts a decrease. The discrepancy with theory is somewhat outside the estimated experimental uncertainty of λ while the experimental trend in λ is less so. Possibly, for the presumably less well-ordered shorter[18] [a] alkane chains, some other effect (such as a λ_{INNER} term or a nonzero reaction entropy[16] or, although we feel this unlikely, an iR_{UNC}-related bias) overwhelms the predicted trend.

Table 2. Rate Constants and Reorganizational Energies λ Obtained from Cyclic Voltammetry at Low Temperatures for $CpFeCpCO_2(CH_2)_nSH/CH_3(CH_2)_{n-1}SH$/Au Monolayers

	chain length		
	$n = 8$	$n = 12$	$n = 16$
reorganizational barrier energy λ (eV)			
expmt[a] λ	0.95 ± 0.03	0.89 ± 0.02	0.80 ± 0.12
calc[b] λ_{CLASS}	0.71−0.73	0.74−0.76	0.77−0.79
calc[c] λ_{2LAYER}	0.76	0.78	0.80
rate constant at 273K			
$k°_{273}$ (s^{-1})[D]	4070	35.5	0.16
$\mu\varrho_{CALC}$ $(eV^{-1}\ s^{-1})$	1.4×10^9	6.5×10^6	1.5×10^4
$\mu\varrho_{ARR}$ $(eV^{-1}\ s^{-1})$	3.7×10^9	1.6×10^7	2.8×10^4

[a] From slope of $\log[k°/k_BT^{1/2}]$ vs T^{-1} plot of $k°$ values derived from Marcus−DOS analysis of cyclic voltammetric ΔE_{PEAK} data taken at potential sweep rates where ΔE_{PEAK} has a weak dependence[8b] on the assumed value of λ. The $\ln(k°/k_BT^{1/2})$ axis accounts for the pre-exponential temperature dependence both of the rate constant[14] and of μ $(=[H_{AB}2/\hbar][\pi/\lambda k_BT]^{1/2})$. Error in λ is taken at the 95% confidence limits. [b] Calculated for 120−180 K from classical dielectric continuum equation for outer sphere reorganizational energy.[15,17] [c] From ref 17c, reduced by 10% to account for difference in ϵ_{OP}. [d] Extrapolated values in $\log[k°/k_BT^{1/2}]$ vs T^{-1} plots, from Figure 4 and refs 8c,d. [e] Calculated from Marcus−DOS theory[14] at 273 K, $\eta = 0$, and λ as in the table.

A central feature of electron tunneling reactions is the expected exponential dependence of rate on distance.[6,15] For ferrocene SAM's, this can be expressed as

$$k° = k°' \exp[-\beta(d - d_0)] \qquad (1)$$

where $k°'$ is the ferrocene heterogeneous rate constant for zero alkane chain length (d_0, i.e., a Au−S−CO_2CpFeCp surface), d is ferrocene−electrode (normal) distance imposed by the alkane chain, and β expresses the overall reaction rate sensitivity to distance. $k°$ results give linear plots over a series of temperatures (Figure 5, Δ, □, ○) that confirm the exponential chain length dependency and give a temperature-independent $\beta = 1.06 \pm 0.08(2\sigma)$ per CH_2.

The β value derived from Figure 5 is in good agreement with other reports[3] on the chain length dependence of ferrocene SAM kinetics in aqueous acid at ambient temperatures. This agreement is significant inasmuch as the aqueous acid studies[3] involved structurally well-ordered and kinetically homogeneous monolayers,[9] as manifested in potential step experiments by linear first-order reaction plots ($\ln[i]$ vs time; slope = k_{APP}), whereas ferrocene SAM's in the low-temperature EtCl/PrCN solvent exhibit[8b−e] nonlinear $\ln[i]$ vs time plots and as much as 8-fold variation in k_{APP} during the reaction of the monolayer. The monolayer population of ferrocene sites in these SAM's and in others based on Ru complexes[10] exhibits a range of

(14) The relation between rate constant and electrode overpotential η used in the cyclic voltammetric analysis is[9]

$$k_{red,ox} = \mu\varrho k_BT \int_{-\infty}^{\infty} \frac{\exp\left[-\left(x - \frac{\lambda \pm \eta}{k_BT}\right)^2 \frac{k_BT}{4\lambda}\right]}{1 + \exp(x)}\,dx$$

where μ is the distance-dependent electronic coupling parameter (see Table 2 footnote *a*), ϱ the density of electronic states in the metal electrode, and k_B the Boltzmann constant.

(15) (a) Marcus, R. A. *J. Phys. Chem.* **1963**, *67*, 853. (b) Marcus, R. A. *J. Chem. Phys.* **1965**, *43*, 679. (b) Newton, M. D.; Sutin, N. *Annu. Rev. Phys. Chem.* **1984**, *35*, 437.

(16) The reaction entropy is assumed zero so that $E_{ACT} = \Delta G^{\ddagger} = \lambda/4$.

(17) (a) Outer sphere reorganizational barriers λ_{CLASS} are calculated from the classical dielectric continuum model,[15] based on dielectric constants extrapolated[8c,d] to the desired temperatures, and assumed mole-fraction weighted dielectric properties for the binary solvent mixture. At 125 K, $\epsilon_{OP} = 2.12$ and $\epsilon_{STAT} = 27.7$. The ferrocene radius is taken[17b] as 3.8 Å. (b) Gennet, T.; Milner, D. F.; Weaver, M. J. *J. Phys. Chem.* **1985**, *89*, 2787. (c) The newer, two-layer calculation of λ_{2LAYER} is by Liu, Y-P.; Newton, M. D. *J. Phys. Chem.* **1994**, *98*, 7162.

(18) (a) Porter, M. D.; Bright, T. B.; Allara, D. L.; Chidsey, C. E. D. *J. Am. Chem. Soc.* **1987**, *109*, 3559. (b) Assumes a monolayer tilted 30° with respect to the surface normal.

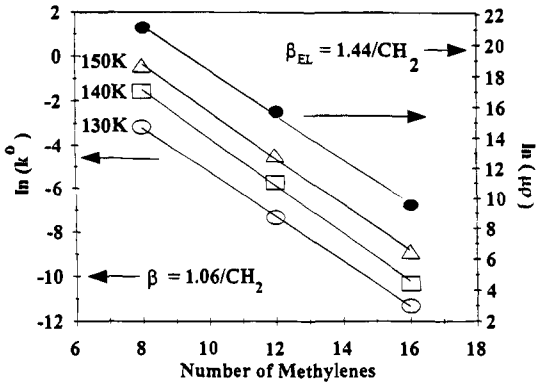

Figure 5. Dependence of $k°$ and of $\mu\rho_{CALC}$ at indicated temperatures on alkane chain length expressed as number of methylene units.

electron transfer rate constants (varying by as much as 4-fold) rather than a single value, i.e., are kinetically disperse. The broadening of cyclic voltammetric waves observed[8] for ferrocene SAM's in EtCl/PrCN is another indicator of kinetic dispersity. The source of the kinetic dispersion has not been definitely established. It may arise[8e] from a distribution of ferrocene formal potentials (i.e., an apparent kinetic dispersion) or of electron transfer distances or values of β or from electrostatic charge buildup.[19] The intrusion of electrolyte and probably solvent that occurs in the EtCl/PrCN medium (indicated by double layer capacitance results[8e]) may be involved. The $k°$ value of a kinetically disperse SAM measured with cyclic voltammetry is an average value but in aqueous acid has been shown[8b] to agree with that of a kinetically homogeneous, but otherwise identical,[9] monolayer in aqueous acid.

The kinetic dispersion clearly reflects subtle chemical differences among the population of ferrocene sites and in turn some level of disorganization in the alkane chain layer. That is, the results in Figure 5 correspond to alkanethiol monolayers that almost certainly contain (defect) alkane chain conformations in addition to the ideal all-trans conformation. In view of the theoretically-expected[6] sensitivity of through-bond tunneling to the presence of, in particular, alkane chain gauche defects, the agreement between the present β for kinetically inhomogeneous monolayers, and previous β results on homogeneous ones,[3] indicates that kinetic inhomogeniety is not connected to a chain length dependency of the incidence of defects in these monolayers. It is possible that defects are localized mainly near or at the outer boundary of the monolayer, so their incidence, and associated kinetic dispersion effects, becomes weakly sensitive to chain length.

The β determined above is only an approximate measure of the electronic coupling through the alkane chain. Sutin et al.[20] have pointed out that β in eq 1 is a composite of the distance dependencies of electronic coupling and of the nuclear factor. Since the latter factor (i.e., λ) varies with chain length (Table 2), the real electronic coupling part of β can be found with a plot (Figure 5) of the pre-exponential $\mu\rho$ term, giving $\beta_{EL} = 1.44 \pm 0.12(2\sigma)/CH_2$, which is 1.1 Å^{-1} based on 1.3 Å/CH$_2$[18a] or 1.3 Å^{-1} based on 1.1 Å/CH$_2$.[18b] This result is somewhat larger than the β_{EL} predicted[6b] for through-bond extended alkane tunneling (0.76 Å^{-1}).

A further test of the consistency of the low-temperature results with those of existing literature can be made by their extrapolation. For example, extrapolation of the $k°$ results to 273 K (Table 2) yields values comparable[21] to those from aqueous acid observations.[3] For the $n = 16$ SAM, extrapolation of Figure 4 to 298 K yields $k°_{298} = 0.34$ s^{-1}, close to the 1.25 s^{-1} result for an identical but kinetically homogeneous SAM[9] in $HClO_4$. Similarly extrapolated $k°_{273}$ values (Table 2), when plotted according to eq 1, give an intercept, corresponding to $n = 0$ in the alkane chain ($k°'_{273}$), of 1.4×10^8 s^{-1} that agrees with the result by Feldberg,[3c] 5.8×10^8 s^{-1}.

Finally, we comment further on effects of kinetic dispersity on measurements of $k°$ from cyclic voltammetry at different temperatures and chain lengths and on the subsequent determination of λ and β. Modeling of kinetic dispersity as a Gaussian distribution of $E°'$ (and thus of $k°$) in cyclic voltammetric and potential step experiments has been fully discussed elsewhere.[8e] Example results pertinent to the present experiments are simulations of cyclic voltammograms at 135 K in which the ferrocene sites exhibit a Gaussian dispersion in $E°'$, with $\sigma(E°') = 55$ mV which was obtained by fitting to the widths of experimental voltammograms. Using parameters of $\lambda = 0.8$ eV and $\mu\rho = 1.48 \times 10^5$ eV^{-1} s^{-1} and a midpoint average rate constant of $k° = 1.78 \times 10^{-4}$ s^{-1} gives simulated cyclic voltammograms which, when analyzed by the method used here,[8b] give average rate constants $k°$ which are almost invariant with potential scan rate (1.03×10^{-3} to 1.24×10^{-3} s^{-1}, over 10 mV/s to 100 V/s, respectively). A similar comparison at 170 K gave apparent $k°$ of 4.2×10^{-2} s^{-1} relative to a midpoint average $k° = 7.7 \times 10^{-3}$ s^{-1}. Thus, this form of kinetic dispersion elevates (5.9- and 5.4-fold, respectively) the measured $k°$ slightly, relative to the average $k°$; i.e., the method slightly favors the "faster" reacting model-dependant midpoint sites. The bias is, however, nearly temperature independent and would cause, in this example, only −4% error in λ and −3-fold error in $\mu\rho$ values derived from an activation plot. These errors are well within experimental uncertainty, so that an $E°'$-based kinetic dispersion should have little or no consequence on $k°$, λ, and $\mu\rho$ determinations by cyclic voltammetry. Further, the lack of any dependence of the $k°$ analysis on potential scan rate in the presence of a Gaussian dispersion in $E°'$ translates to a similar insensitivity to chain length since both potential scan rate and chain length increases produce increases in ΔE_{PEAK}. This was confirmed by simulations, so we additionally conclude that the kinetic dispersion should have no significant influence on the determined value β.

Acknowledgment. This work was supported in part by grants from the Office of Naval Research and the National Science Foundation. We thank Larry S. Curtin for preparing $CpFeCpCO_2(CH_2)_{12}SH$, Professor C. E. D. Chidsey for helpful advice, and Stephen Woodward of the UNC Electronic Shops for design of potentiostat filter and feedback modules.

JA943173V

(19) (a) Smith, C. P.; White, H. S. *Anal. Chem.* **1992**, *64*, 2398. (b) Creager, S. E.; Weber, K. *Langmuir* **1993**, *9*, 844.

(20) Isied, S. S.; Vassilian, A.; Wishart, J. F.; Creutz, C.; Schwarz, H. A.; Sutin, N. *J. Am. Chem. Soc.* **1988**, *110*, 635.

(21) At 298 K, $\epsilon_{OP} = 1.78$ for EtCl/PrCN and 1.87 for water. Since ϵ_{op} dominates the calculation of λ_{CLASS}, λ_{CLASS} should be similar in the two solvents.